Neuronal basis of visual perception and attention in visual and frontal cortex

Pooresmaeili, A.

2010

document version
Publisher's PDF, also known as Version of record

Chapter 3: Neuronal activity in area V1 during contour grouping conforms to a growth-cone model of object-based attention

Arezoo Pooresmaeili and Pieter R. Roelfsema

Summary

Attention can select elements of spatially extended objects and group them into coherent representations, but the processes responsible for object-based attention have remained unclear. Shape-selective neurons in higher areas of the visual cortex could contribute to object-based attention by providing feedback to lower areas to enhance the representation of image elements that belong to a relevant shape (Van der Velde and de Kamps, 2001). Another possibility is that attention gradually spreads according to the Gestalt rules, successively adding new elements to a growing object representation. Here we investigated the dynamics of object-based attention by recording the activity of area V1 neurons in a contour grouping task. Our results show that attention gradually spreads across the object representation as neuronal responses evoked by contour elements further along a relevant curve are enhanced at progressively later times, while responses evoked by the initial segments of the curve stay at an enhanced level. The speed of the attentional spreading process decreased at locations where the relevant curve came close to an irrelevant one. Our findings inspire a "growth-cone" model where attention spreads at multiple spatial scales by enhancing the responses of neurons with differently sized receptive fields, at a pace of approximately 50ms per receptive field.

Introduction

The typical visual scene that we perceive is rich in content with a large number of objects that can be in each other's close proximity and may be seen on a complex background. We usually identify and act upon one or a few objects of interest at a time, and our visual system should group the image elements that belong to these objects and segregate them from other objects and the background. This perceptual grouping process is not only important for object recognition, but also for our visually guided actions. If we grasp an object, for example, it is essential to place our fingers on surfaces of the same object. Perceptual grouping is therefore a crucial component of many aspects of visual processing.

Various mechanisms have been proposed for perceptual grouping ; (reviewd by Roelfsema, 2006). One of these mechanisms is the activation of neurons in higher areas of the visual cortex that are tuned to complex shapes and object categories, like the inferotemporal cortex (Brincat and Connor, 2004; Oram, 1994; Tanaka, 1993; Thorpe et al., 1996). The activation of neurons tuned to the shape of, for example, an animal can cause the animal's legs, head and trunk to be grouped in perception. If the visual scene contains multiple

extended objects, then their representations engage in a competitive interaction (Desimone and Duncan, 1995) (Figure 1A), until the representation of the relevant object is enhanced over the representation of irrelevant objects (Moran and Desimone, 1985; Sheinberg and Logothetis, 2001). At a psychological level of description, object-based attention is directed to the relevant shape (Baylis and Driver, 1993; Duncan, 1984; O'Craven et al., 1999b; Vecera et al., 2000; Vecera et al., 2001; Vecera and Farah, 1994). The selection of a shape in the inferotemporal cortex can also have consequences for the representation of more elementary features in lower visual areas. Theories suggest that inferotemporal neurons that win the competition feed back to also enhance the relevant object's representation in these lower areas (Fukushima, 1988; Van der Velde and de Kamps, 2001; Vecera and Farah, 1994). Studies of perceptual grouping observed correlates of object-based attention in area V1, at the lowest level of the visual cortical processing hierarchy (Li et al., 2006; Roelfsema et al., 1998). For example, in a contour grouping task where monkeys had to mentally trace a target curve (Figure 2A), V1 activity evoked by this curve was enhanced over the activity evoked by an irrelevant curve. If this response enhancement is primarily caused by shape selective neurons in higher visual areas that feed back to lower levels, then the feedback might enhance the representation of all contour elements of the relevant curve at approximately the same time (Figure 1A).

However, the activation of shape selective neurons in higher visual areas is presumably not the only neuronal mechanism for object-based attention. Image elements that do not belong to familiar objects also group in our perception if they are related to each other by low-level grouping cues (Gestalt rules) (Koffka, 1935; Wertheimer, 1923). We see a curve in any set of contour elements in each others' good continuation, i.e. if they are connected and collinear, and it is unlikely that there are neurons in higher visual areas tuned to the shape of all possible curves (Roelfsema and Singer, 1998). Perceptual grouping of unfamiliar curves could take place in early visual areas where neurons code the individual contour elements, provided they can somehow signal that they code elements of the same curve. The enhancement of neuronal responses evoked by a relevant curve in low level areas could act as such a label, tagging the neuronal responses evoked by the image elements of the same perceptual group (Roelfsema, 2006). If the Gestalt grouping cues are a dominant factor in contour grouping, then it is predicted that the response enhancement starts at the initially cued parts of an object and then spreads gradually across successive contour elements of the relevant object (Figure 1B). This mechanism would explain why the time required to group contour elements into an elongated shape increases linearly with the length of the curve, i.e. with number of contour elements to

be grouped in perception (Jolicoeur et al., 1991a). Moreover, human observers indeed gradually spread their attention over a relevant curve during contour grouping (Houtkamp et al., 2003; Roelfsema et al., 2000; Scholte et al., 2001).

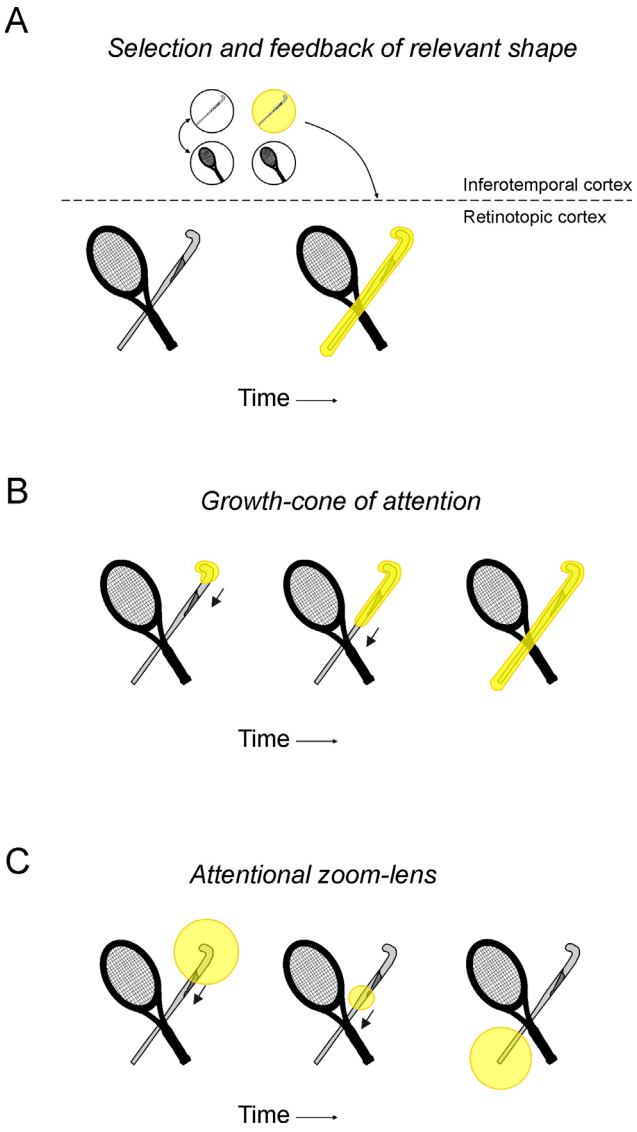

Figure 1. *Three models for the time course of attention shifts for spatially extended objects*

A) Shape-selection model. This model assumes that the representations of the shapes of the two objects compete in higher cortical areas. When one of these objects is selected, feedback enhances the representation of the image elements of the selected shape in early visual areas.

B) Growth-cone of attention model. The model holds that attention gradually spreads across the attended object. The attentional 'growth-cone' adds new image elements to the set of attended elements.

C) Attentional zoom-lens model. This model assumes that an attentional focus of varying size shifts along the relevant object.

A role for object-based attention in the curve tracing task of Figure 2A is not undisputed, however. Jolicoeur and his co-workers (Jolicoeur et al., 1991a; McCormick and Jolicoeur, 1991) suggested that a variably sized "zoom-lens" of attention (Eriksen and St James, 1986; Posner, 1980) is shifted along the traced contours (Figure 1C). They demonstrated that this model accurately predicts the pattern of reaction times if it is assumed that tracing time depends on the total number of the shifts of the zoom-lens needed to traverse a curve. "Zooming" is a critical feature of this model because it explains why speed of tracing

in human perception depends on the distance between a target curve and the distracting curves. If the curves are far apart, the zoom-lens can be large and a few shifts suffice for a long curve. If the curves are nearby, however, the zoom-lens contracts and tracing speed decreases, just as is observed in human psychophysics (Jolicoeur et al., 1991b; McCormick and Jolicoeur, 1991). Zooming also explains why curve-tracing is scale invariant: response times do not depend on viewing distance (Jolicoeur and Ingleton, 1991). If the observer comes closer to an image and sees it at a higher magnification, the length of the curve that has to be traced as measured in degrees of visual angle increases, but the size of the zoom-lens operator increases proportionally, so that the total processing time remains constant.

The distinction between the zoom-lens and growth-cone model maps onto a classical distinction between spatial attention and object-based attention (Duncan, 1984; Kanwisher and Driver, 1997). The zoom-lens is a spatial focus of attention that enhances the representation of only a small segment of the target curve at a time. Contour elements at the start of the curve are no longer attended when the zoom lens has moved on. The zoom-lens model therefore does not give rise to object-based attention nor to perceptual grouping of all the contour segments of the target curve. The spreading attention model, in contrast, describes the dynamics of object-based attention and eventually labels all image elements of a single object. A psychophysical study demonstrated that attention stays on the beginning of the target curve during curve tracing in support of the attentional spreading model (Houtkamp et al., 2003), but a later study argued in favour of the zoom-lens model (Crundall et al., 2008) although that study was recently criticized on methodological grounds (Roelfsema, Houtkamp & Korjoukov, *subm*).

So far, object-based attention has been mainly studied at the behavioral level, and it is difficult to resolve the time-course of attention shifts with purely behavioral techniques. Here we will therefore investigate the dynamics of object based-attention in the primary visual cortex during a contour grouping task to address the following questions: (1) Does the response enhancement stay on the initial segments of a target curve? (2) Is there a gradual increase of the latency of the attentional response modulation along a traced curve? (3) Does the progression of the attentional labeling process depend on the distance between the target curve and other objects in the display?

Results

Two macaque monkeys performed the curve tracing task depicted in figure 2A. At the beginning of a trial, the monkeys directed their gaze to a fixation point in the centre of a display. After 300 ms, two curves with two larger circles at their ends were displayed on the screen while the monkeys maintained fixation. One of the two curves was connected to the fixation point (the target curve) and the task of the monkeys was to locate the circle at the other end of this curve while ignoring the other curve that was a distractor. After 600 ms, the fixation point disappeared and the monkeys had to indicate their choice by making an eye movement to the larger circle at the end of the target curve.

Figure 2B shows a set of stimuli that were used during one of the recording sessions. The stimuli that are shown above each other are called "complementary" because the target and the distracter curves are interchanged by switching the connection with the fixation point. The two curves came close to each other at a location which will be referred to as the "critical zone" (blue square in figure 2B). At the critical zone, the curves either intersected each other or stayed apart (non-intersection). We manipulated the difficulty of the task by varying the gap between the curves (from 0.15° to 1.8° in visual degrees) if they did not intersect or by changing the angle of intersection (from 18° to 90°) if they did. The difficulty manipulation was effective because the monkeys made more errors if the two curves were closer to each other in case of a non-intersection or if they intersected each other at a smaller angle as has been shown previously (Roelfsema and Spekreijse, 2001).

We recorded multiunit spiking activity with chronically implanted electrodes from a total of 82 recordings sites in area V1 while the monkeys performed this task. Of these recording sites, 44 came from two hemispheres of one monkey, and 38 from one hemisphere of another monkey. We observed variable strengths of attentional modulation across our recording sites where some sites were strongly modulated by attention and some were not (Supplementary figure S1). Since our analyses will focus on measurements of the latency of response modulation, we included only recording sites that were significantly modulated by attention (53 sites; 27 sites from monkey R and 26 sites from monkey G). The location of the critical zone was kept constant within a recording session but it differed between sessions because the stimuli were adapted to the receptive fields of the recorded neurons. The receptive fields of the recorded neurons were either between the fixation point and the critical zone (less eccentric than the critical zone) or between the critical zone and the saccade targets (more

eccentric than the critical zone) and we will refer to these receptive field locations as "close" and "far", respectively (Figure 2B).

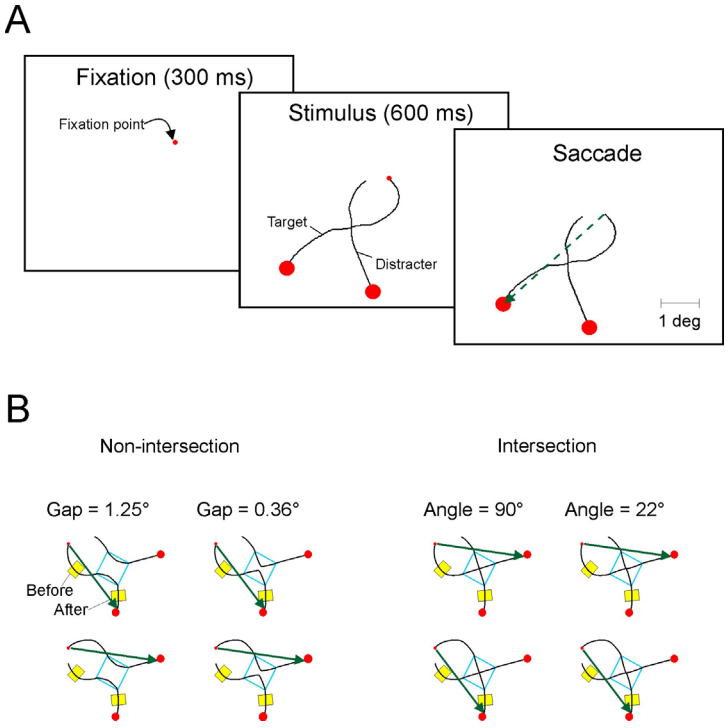

Figure 2. *The curve tracing task*

A) Sequence of events in the curve tracing task. The monkeys directed their gaze to the fixation point. The stimulus appeared after 300 ms of fixation and after an additional delay of 600 ms they had to make an eye movement to the red circle at the end of the target curve that was connected to the fixation point.

B) Different stimulus configurations that were used in a single recording session. The stimuli differ at two locations, as the fixation point can be connected to either of the two curves and the contour segments within the critical zone (the blue square, not shown to the monkey) varied between stimuli so that the curves either intersected each other or stayed separate. We varied the distance between the curves if they did not cross each other and the angle of intersection if they did. The receptive fields of the neurons were either before or after the critical zone.

Neuronal responses evoked by close and far contours of the target curve

We examined how the timing and duration of the contour selection process depends on receptive field location and on the distance between the two curves at the critical zone. Figure 3 shows the responses of two example recording sites in area V1 recorded within the same session. One of the recording sites had its receptive field before the critical zone (upper row in Figure 3) and the other recording site after the critical zone (lower row in Figure 3). We compared the neuronal responses between complementary stimuli with a total of four stimulus

configurations at the critical zone: a non-intersection with a gap size of 0.33° or 1.3°, and an intersection with an angle of 22° or 90°. The neurons first showed a transient response which did not distinguish between the target and the distracter curve. After this initial response, activity evoked by the target curve was enhanced relative to activity evoked by the distracter curve ($P < 0.05$, Mann–Whitney U-test) as described previously (Roelfsema et al., 1998; Roelfsema and Spekreijse, 2001). In order to estimate the onset time of the attentional modulation, we fitted a function to the difference between the responses to the target and the distracter curves and defined the latency as the time when this function reached 33% of its maximum (Roelfsema et al., 2003) (see Methods). The onset of the attentional modulation for the recording site with a receptive field before the critical zone was relatively constant across stimuli and ranged from 106 to 138 ms. The onset of the attentional modulation was more variable for the recording site with a receptive field after the critical zone, and ranged from 177 ms for the non-intersection with a gap size of 1.3° to 347 ms for the gap-size of 0.33°, while the modulation latency for stimuli with an intersection was intermediate.

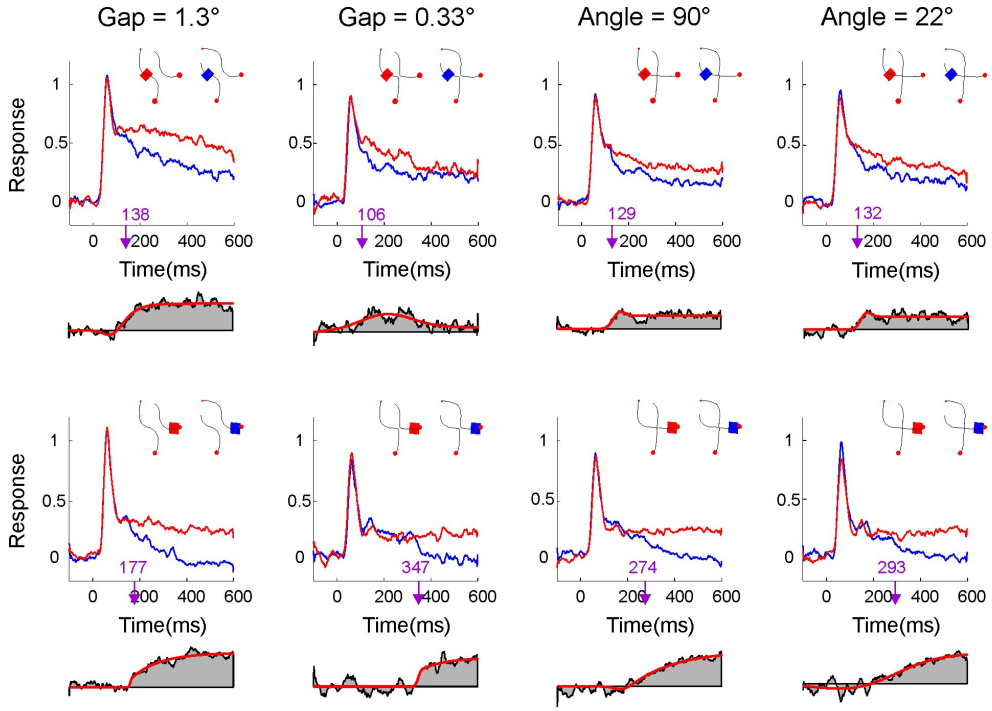

Figure 3. *Latency of attentional modulation of V1 neurons with close and far receptive fields*

A) Responses of two example sites that were recorded in the same session. The receptive field of one site was before (upper panel, close receptive field) and the other was after the critical zone (lower panel, far receptive field). The neuronal responses evoked by the target curve (red traces) are compared to those evoked by the distracter curve (blue traces). The number on the X-axis denotes the latency of response modulation measured by fitting a function (red curve) to the difference between responses to the target and the distracter curves (shown below each graph).

Temporal profile of attentional modulation at the initial segments of the target curve

The data of Figure 3 illustrate a number of findings that are representative for the entire population of recording sites. First, the enhancement of neuronal responses evoked by the initial segments of the target curve tended to be maintained for the entire duration of a trial. In the example of Figure 3, the attentional modulation stayed at a relatively constant level in three of four stimulus conditions, although there was a reduction in the strength of attentional modulation for the non-intersection with a gap of 0.33° towards the end of the trial. The maintenance of attentional modulation for contour elements at the beginning of the target curve was also observed across the entire population of recording sites with a receptive field before the critical zone (*N*=18) (Figure 4A, upper panels). At the population level, the attentional modulation at the start of the target curve was maintained until the end of the trial, for all stimulus configurations. To investigate the stability of the attentional modulation across time for the close recording sites, we compared the strength of attentional modulation in an early time window (100-200 ms after stimulus onset) to that in a later time window (500-600 ms). We quantified the strength of the modulation with the *d'*, which is a measure for the reliability of the difference in response strength evoked by target and distractor curve on single trials (see the experimental procedures). It can be seen in Figure 4B that the *d'* values in these two time windows were similar (P> 0.3, paired t-test) indicating that the attentional modulation did not retract from the initial segments of the target curve.

Latency of attentional modulation before and after the critical zone

In the example of Figure 3, the attentional modulation of the response of the recording site with a close receptive field occurred earlier than that for the recording site with a far receptive field. We observed comparable timing differences at the population level (Figure 4A). The modulation latencies of neurons coding the more distal curve segments were longer than those for neurons coding the initial curve segments. We tested the significance of the difference in timing of the attentional effect with a bootstrapping method (see the Supplementary Information). If the stimulus had a non-intersection with a large gap (the gap size ranged from 0.15° to 1.8° in visual degrees), the attentional modulation for neurons with close receptive fields occurred at a latency of 126ms, 38ms before neurons with a far receptive field that had a latency of 164ms (Figure 4A) (bootstrapping test, $P<10^{-3}$, see Methods). This difference in the timing of the modulation increased to 127 ms when the gap was narrower ($P< 10^{-10}$). In case of an intersection, the timing differences before and behind the critical zone were 49 ms

and 89 ms for intersections with a large and small angle (the intersection angle ranged from 18° to 90°), respectively (Figure 4A) ($P< 0.01$ in both cases). We next investigated whether these latency differences could also be observed when we evaluated the distributions of attentional latencies at individual recording sites. Figure 5A illustrates the cumulative distribution of modulation latencies in response to the different stimulus conditions. In case of a non-intersection, the modulation latencies were significantly shorter for the close receptive fields than for the far receptive field, an effect that was significant when the gap was large and also when the gap was small ($P < 0.01$ in both cases, Mann-Whitney *U*-test). We observed a similar effect for the stimuli with an intersection as modulation latencies for recording sites with close receptive fields were shorter than those for sites with far receptive fields, if the angle of the intersection was large as well as if it was small ($P<0.01$ in both cases, Mann-Whitney *U*-test).

Effects of gap-size and intersection angle on attentional modulation latency

In the example of Figure 3, the timing of the modulation of neurons with a close receptive field did not depend strongly on the angle of the intersection or on the gap between non-intersecting curves, whereas the modulation latency of neurons with a far receptive field increased for stimuli with a small gap between the curves and for stimuli with a sharp intersection. To better characterize these effects, we compared the timing differences at the population level (Figure 4A). If the receptive field was before the critical zone, there was an unexpected trend for smaller gaps to *reduce* the modulation latency from 126 ms to 113 ms, but this effect was not significant (P=0.07, bootstrapping test). A sharper angle of the intersection had little effect on the modulation latency for neurons with a receptive field before the critical zone (128 vs. 127 ms, P>0.45). In contrast, the attentional modulation of the responses of neurons with a receptive field after the critical zone was increased from 164 to 240 ms when the gap size of a non-intersection was decreased (P<0.001, bootstrapping test). A sharper angle of an intersection between the two curves also tended to increase the latency of the modulation, from 177 for the larger angles to 216 ms for the smaller ones, but this effect was not significant (P = 0.092).

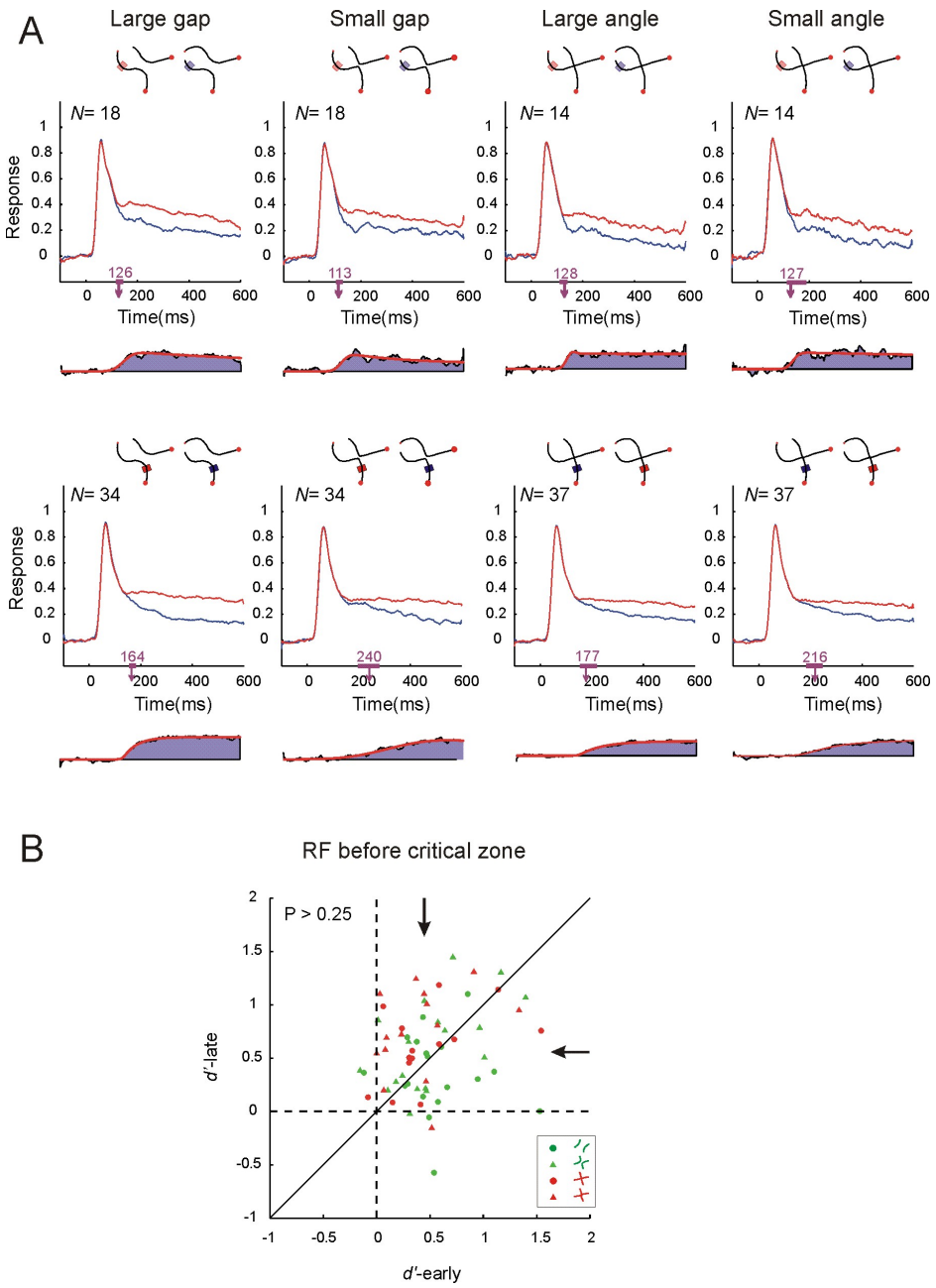

Figure 4. *The population responses of V1 neurons in the contour grouping task:* A) The population responses of neurons with close receptive fields (upper panel) and far receptive fields (lower panel). Population responses are shown for stimuli with a non-intersection with a large or small gap, and for stimuli with intersections with a large or small angle. The latency of the response modulation was measured by fitting a function (red curve) to the difference between responses evoked by the target and distracter curve. The number on the X-axis denotes the estimated latency and the bars on the X-axis the 95% confidence interval. B) Comparison of the strength of attentional modulation (*d*') in an early (100-200ms after the stimulus onset, abscissa) and late time window (500-600ms, ordinate). The *d*' values were not significantly different (*P*>0.3, paired t-test) indicating that the response enhancement for initial segments of the target curve remains at a relatively stable level until the end of the trial. Arrows show the medians of the distributions.

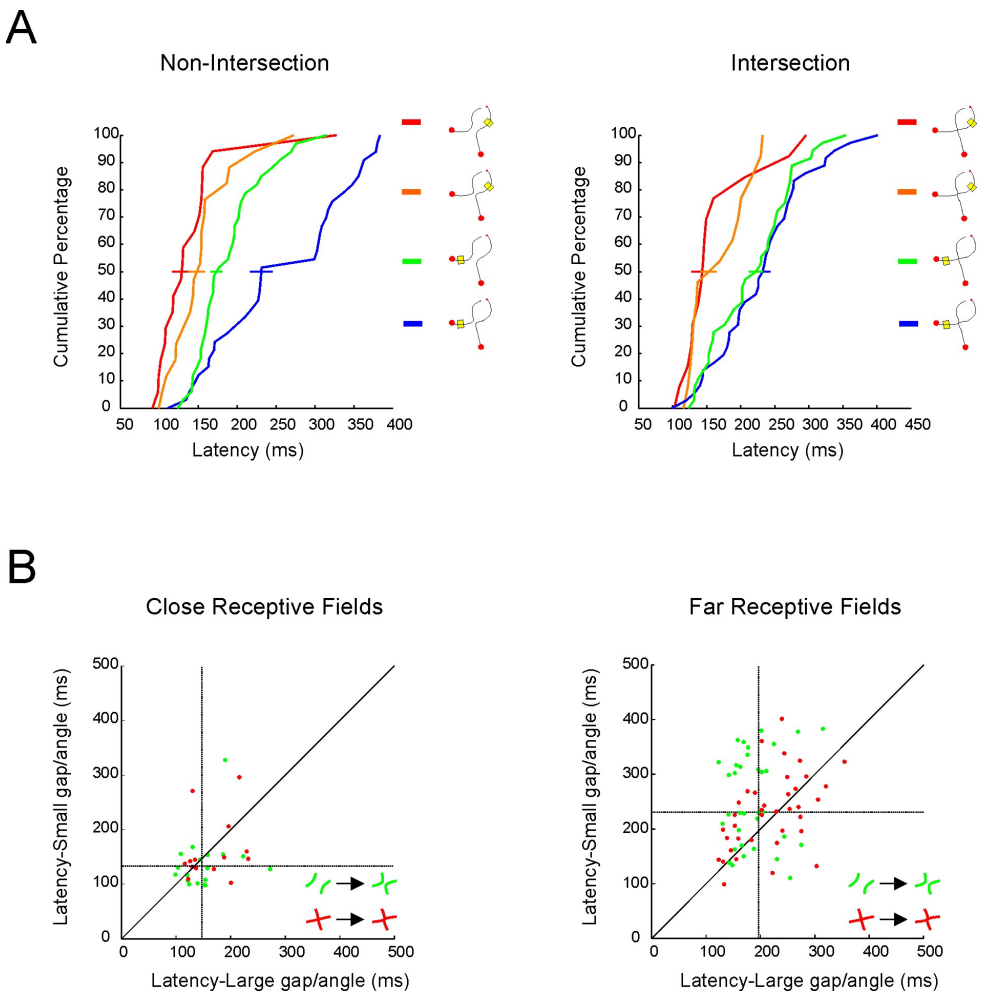

Figure 5. Distribution of the modulation latencies

A) The cumulative distribution of the latencies is shown for the non-intersections with small and large gaps and for the intersections with large and small angles. The response modulation occurred later in time when the receptive fields of the neurons were further along the curve (all *P*s< 0.01, paired t-test). When the gap of a non-intersection became smaller the responses were modulated later in time, but only for neurons with receptive fields distal to the critical zone (P< 0.001). The angle of an intersection did not have a significant effect on the modulation latency of neurons with either close or far receptive fields (P>0.1).

B) Distribution of the modulation latencies across individual recording sites. The latencies of the response modulation for small gaps and sharp intersections (ordinate) are plotted against the latencies for large gaps and intersections with large angles (abscissa) for close (left panel) and far (right panel) receptive fields. Green and red data points show modulation latencies for stimuli with and without an intersection, respectively. The dashed lines denote the median of the modulation latency.

We obtained similar results when we investigated the modulation latencies across the individual recording sites (Figure 5B). The modulation latencies of neurons with a receptive field before the critical zone were not significantly affected by a decrease in the gap-size of a non-intersection or the angle of an intersection (both *P*s >0.1, *U*-test). The responses modulation of neurons with a receptive field after the critical zone were significantly delayed

if the gap-size of a non-intersection was decreased ($P< 0.001$), however a sharper intersection did not significantly delay the modulation latency ($P>0.4$).

The findings described so far are largely consistent with the attentional spreading model. We found that attentional modulation is maintained on the initial contour elements of the target curve, and that the attentional modulation for the early contour elements of the target curve precedes the modulation of the more distal parts. However, we also obtained a result that is reminiscent of the zoom-lens model described in the introduction because the speed of propagation was found to be decreased if the two curves come in close proximity at the critical zone. According to this model, the zoom-lens contracts and tracing slows down at locations where the curves are nearby. And yet, the zoom-lens model does not predict that the attentional modulation stays at the start of the target curve. Our results therefore inspire a new model that combines the ideas of attentional spreading and zooming that we call the 'growth-cone' model of object-based attention. According to the new model, attention spreads across the target curve, and we call the location where attention actively spreads the attentional growth cone (Figure 6A). We hypothesize that the growth-cone can be large and attention spreads rapidly if the target curve is far from other elements in the display (Figure 6A, upper row), while it contracts and slows down if the target curve comes close to a distractor (Figure 6A, lower). At the end of the task, all the contour elements of the target curve would be labelled by attention. A model for the implementation of such a growth cone model in the visual cortex will be proposed in the discussion.

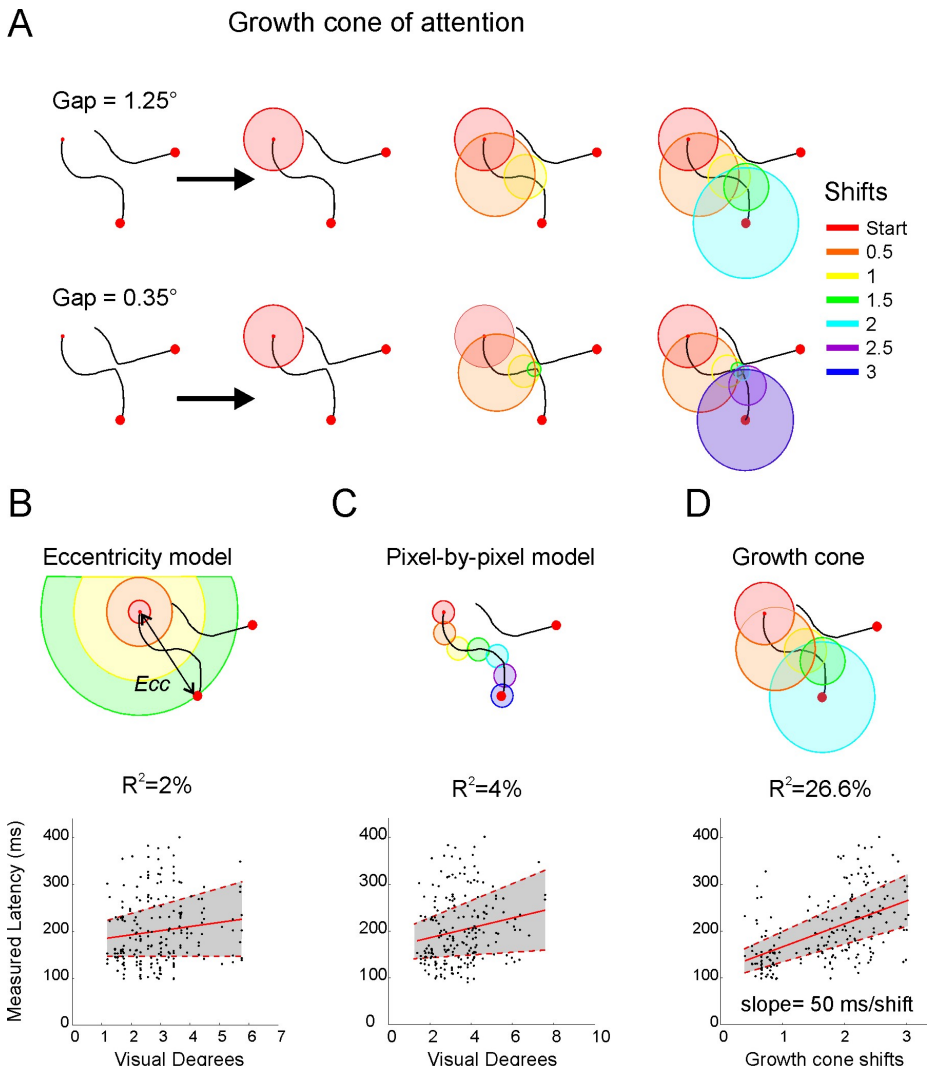

Figure 6. Growth-cone model of attention

A) Schematic representation of the propagation of the attentional response modulation according to the growth-cone model for curves with a large (upper panel) and small gap (lower panel). The growth-cone starts at the fixation point and causes attention to spread across the target. The coloured circles illustrate the location of the growth-cone after shift of half a diameter of the cone. The size of the growth cone is adjusted so that it never includes segments of the distracter curve. If the distance between curves is smaller the growth cone has to shrink more and additional shifts are required.

B) The eccentricity model holds that the onset of attentional modulation depends only on the eccentricity of the receptive field. The lower panel shows the linear regression between this model and the measured modulation latency. Red curves show the regression line (solid red line) and the grey regions shows the 95% confidence interval for the regression line (dashed red line). The goodness-of-the-fit (R-square) for each model is shown.

C) In the length-integration model attention starts to spread from the fixation point to the other segments of the target curve at a constant speed (in degrees per second).

D) Growth cone model where the speed of propagation depends on the distance between curves.

To investigate whether the growth-cone model gives a useful description of the data, we compared it to two other models that might explain the latency results. The first model was an 'eccentricity model' that will be used as a baseline against which we will compare the other two models. The eccentricity model assumes that the latency of the attentional modulation only depends on the eccentricity of the receptive field. In our displays the target curve started at the fixation point and the contour elements further along the curve had increasing eccentricity. The receptive field's location on the target curve was therefore correlated with its eccentricity. The eccentricity model estimates the time $t(A)$ of the onset of the modulation for a receptive field at location p_A as follows:

$$t(A) = t_C + \alpha Ecc(A) \qquad (1)$$

Where t_C is a constant time required to initiate the tracing process, $Ecc(A)$ is the eccentricity of p_A, and α is a constant in degree/s that specifies how the timing of the attentional modulation depends on the eccentricity of the receptive field. To evaluate the model, we calculated the linear regression between eccentricity and the measured modulation latency of recording sites in the stimulus configurations of figure 2B so that a single recording site could contribute up to four data points (Figure 6B). The correlation between latency and eccentricity was weak $\rho = 0.13$ and did not reach statistical significance (paired *t*-test, $P = 0.063$).

Our second model was a 'pixel-by-pixel' spreading model first described by Jolicoeur et al. (Jolicoeur et al., 1991a) that assumes that the tracing process proceeds at a fixed speed, which does not depend on the distance between the curves. Thus according to this model, the onset of the attentional modulation depends linearly on the arc length of the curve between the fixation point and the receptive field (Figure 6C). The time required for the propagation of the enhanced response from the fixation point to a point p_A on the target curve is estimated as follows:

$$t(A) = t_C + vL(A) \qquad (2)$$

Here $L(A)$ is the arc length of the curve between the fixation point and point p_A, and v is tracing speed in degree/s. The linear regression of this model was significant ($P<0.01$) with a slope of 10.5 deg/ms and an intercept of 165 ms. However, the fit explained only 4% of the

variance in the data and had a correlation coefficient of 0.2 and a bootstrapping test revealed that the fit of the pixel-to-pixel model to the data was not significantly better than the fit of the eccentricity model ($P > 0.05$).

The third model is the growth-cone model where the speed of the attentional spreading process depends on the distance between the target and the distractor curve (see also Jolicoeur et al., 1991b; McCormick and Jolicoeur, 1994) . The growth-cone is scaled such that it does not include points of the distracter curve (Figure 6A). It is large at locations where the curves are far apart and it shrinks if the curves come close to each other. To estimate the size of the growth-cone at each point p_A of the target curve, we measured the distance between p_A and the nearest point of the distractor curve. The time required for the tracing process to reach a point p_A is as follows:

$$t(A) = t_C + \beta L_{Norm}(A) \tag{3}$$

Here, β is the time (in ms) required by a single shift of the growth cone, and $L_{Norm}(A)$ is the arc length of the curve between the fixation point and p_A, measured as the number of shifts over a distance that is equal to the growth cone's diameter. Thus, L_{Norm} is defined as follows:

$$L_{Norm}(A) = \sum_{A'=1}^{A} \frac{\left\| p_{A'} - p_{A'-1} \right\|}{Diam(A')} \tag{4}$$

Where the sum is taken over subsequent points $p_{A'}$ on the target curve up to the point p_A, p_0 is the fixation point, $\|p_{A'}-p_{A'-1}\|$ is the Euclidean distance between points, and $Diam(A')$ is the diameter of the growth-cone at point $p_{A'}$, which equals two times the distance to the nearest point on the distractor curve. Equations 3 and 4 could explain why decreasing the distance between the target and the distracter curve protracts the attentional modulation of neuronal responses evoked by the subsequent curve segments (compare upper and lower panels in Figure 6A). We made an additional assumption to obtain fits of this model for stimuli with an intersection. At an intersection, the distance between the curves becomes zero and the growth cone shrinks to a point that does not cross over to the other side. We therefore assumed that the growth cone's diameter could not be smaller than a fixed value (1°). We note that the precise value of this lower limit on the size of the growth cone within a reasonable range

(between 0.6 and 2 degrees, see Supplementary Figure 2) had little influence on the quality of the fit.

To estimate t_C and β, we performed a linear regression between the predicted and measured modulation latencies (Figure 6D) and observed a correlation coefficient of 0.51 ($P<10^{-14}$). The growth-cone model accounted for 26.6% of the variance in attentional latency, which was significantly better than the pixel-by-pixel and the eccentricity model (both Ps<0.01, bootstrapping test). The slope β of the regression line provides a measure for the speed of the spread of attention as it estimates the time required for a single shift of the growth cone. We obtained a β of 49ms per shift (95% confidence interval 38-60 ms), while the offset time t_C was 118ms. We obtained similar estimates when we evaluated the data of the monkeys separately, with a slope of 45ms/shift for monkey G and a slope of 55ms/shift for monkey R (see Supplemental Material).

So far we used an arbitrary criterion for the latency of the modulation, defining it as the point in time where the modulation reached 33% of its maximal amplitude. We next considered the possibility that the attentional shift time might depend on the criterion. We therefore repeated our analysis using criteria of 25% and 50% of the maximum as onset time of the modulation, and obtained slopes β of 46 and 59 ms per shift, respectively. In the Supplementary Information, we outline why our latency estimate has advantages over other latency measurement that rely, for example, on the significance of the difference in the response evoked by the target and distractor curve. Nevertheless, to ensure that our estimate of the speed of attentional propagation is robust, we also evaluated a latency criterion that is based on significance, taking the first of three consecutive time bins with a significant (P<0.05) difference between responses as the onset time and obtained a slope β of 49ms per shift. We conclude that our estimate of 50ms per shift of the growth cone does not depend strongly on the precise method used to determine the onset of attentional modulation.

The three models of Figure 6B-D have correlated variables as the normalized arc length $L_{Norm}(A)$ of equation 3 is correlated with the non-normalized arc length $L(A)$ of equation 2, which in turn is correlated with the eccentricity $Ecc(A)$ of equation 1. We computed partial correlations to examine the fit of each of the three models when the variance explained by the other models had been removed. The partial correlation coefficient of the eccentricity model was 0.06, which did not differ significantly from zero (P>0.15, F-test). Similarly, the partial correlation of the pixel-by-pixel model was -0.11 which was also not significantly different from zero (P>0.1). In contrast, the partial correlation coefficient of the

growth cone model was 0.48, which was significantly larger than zero ($P<10^{-10}$) and this model accounted for 20% of the residual variance.

Discussion

Here we have investigated the dynamics of object-based attention in area V1 of monkeys performing a contour grouping task. We obtained a number of new and unexpected results regarding the dynamics of object-based attention. Firstly, we found that the neuronal correlates of visual attentional occur progressively later for contour elements that are further along a traced curve. Secondly, the neuronal response enhancement caused by attention persists for the initial contour elements of a curve until the entire curve is labelled by attention. Thirdly, variations in the distance between the target and the distracter curve influence neuronal modulation latencies, but only for neurons coding contour elements distal to the distance manipulation. The spread of attention is slowest at locations where the target curve comes close to a distractor curve, which is consistent with previous psychophysical results indicating that the speed of curve tracing in human observers also depends on the distance between curves (Jolicoeur et al., 1991b). Fourth, we found that a growth-cone model of object based attention captures most aspects of our data and we estimated the needed for a shift of attention to an adjacent location within an object to be approximately 50ms.

A growth-cone model of object-based attention in contour grouping

We and others (Grossberg and Raizada, 2000; Roelfsema, 2006; Roelfsema and Singer, 1998) have previously suggested that contour grouping could be implemented in the visual cortex as the propagation of an enhanced response between neurons with nearby and well aligned receptive fields, which are tuned to the same orientation. Anatomical studies have demonstrated that horizontal connections indeed preferentially link neurons with receptive fields in collinear configurations, in accordance with the Gestalt grouping rule of good continuation (Bosking et al., 1997; Schmidt et al., 1997). Models of cortical processing usually assume that horizontal connections are modulatory and interact with the visual input in a multiplicative manner; so that they amplify the responses of neurons that are driven well by the visual stimulus but have little influence on neurons not driven by input from the LGN (Fukushima, 1988; Grossberg, 1999). A model based on these principles has been illustrated in Figure 7A, with V1 neurons that can propagate an enhancement of neuronal activity through horizontal connections. The neurons in Figure 7A that are well driven by the stimulus

are shown as grey squares and the neurons not activated by the stimulus as white squares. The multiplicative interaction between horizontal connections and the input dictates that only neurons that are well driven can participate in the propagation of an enhanced response, and we have indicated the horizontal connections between active neurons in orange. The yellow labelling in Figure 7A illustrates how such a model would propagate an enhanced response across all the neurons that code contour elements of the same curve. We note that this model behaves as the pixel-by-pixel model described above (Figure 6C) because the speed of propagation is constant and independent of the distance between curves.

In contrast, our results indicate that the response enhancement propagates slowly if curves are close together and that it speeds up if they are far apart, thereby supporting previous studies showing that curve tracing is a scale-invariant process (Jolicoeur and Ingleton, 1991). How could the visual cortex achieve this scale invariance? One possible solution that comes from computer vision (Edelman, 1987) but that could also be implemented in the visual cortex (Roelfsema and Singer, 1998) has been illustrated in Figure 7B. The main idea is that the propagation of the enhanced response can take place in visual areas at multiple levels of the visual cortical hierarchy where neurons have different receptive field sizes. When the two curves are far apart, neurons at higher levels of cortical hierarchy (for example area V2 or V4) with larger receptive fields will participate in the propagation of the enhanced response. These receptive fields cover a larger segment of the target curve and horizontal connections in these areas interconnect neurons representing spatial locations that are farther apart so that the speed of propagation as measured in degree/s increases accordingly. This faster progress attained in higher areas could be fed back to lower areas, and this could explain why the propagation speed observed in V1 is higher than could be achieved by the V1 horizontal connections alone.

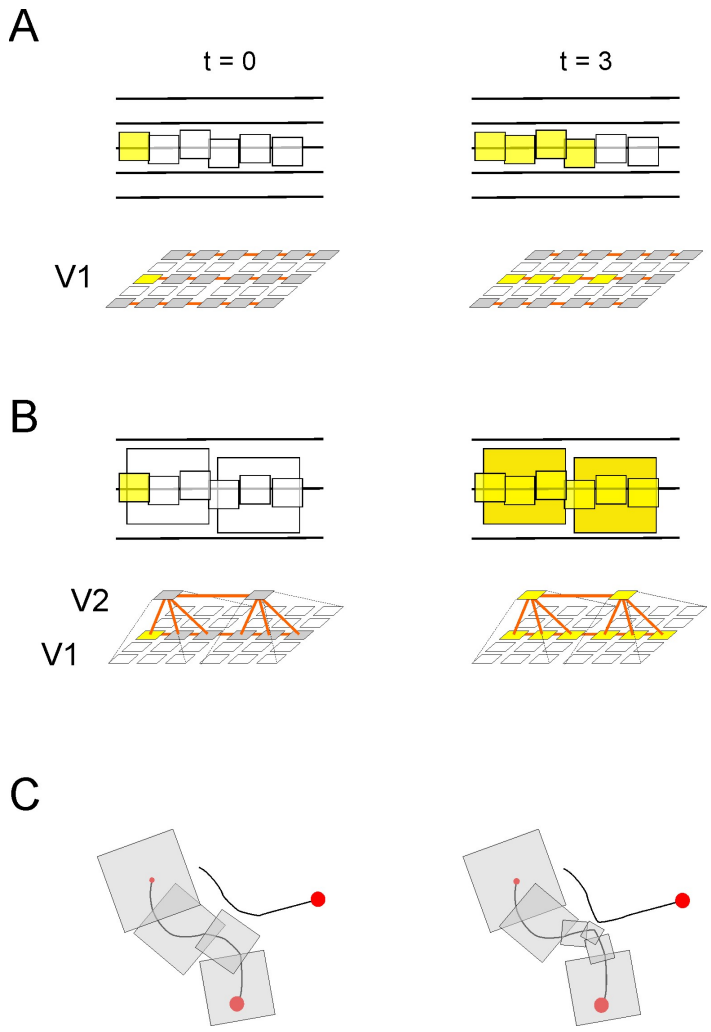

***Figure** 7. Neuronal implementation of the attentional growth-cone model*

A) The contour grouping process can be implemented as the spread of an enhanced response through horizontal connections between neurons with adjacent RFs. The upper panel shows the propagation of the response enhancement in retinotopic coordinates. The squares denote the RFs of neurons in area V1. The lower panel shows a set of neurons in area V1 activated by the stimulus that are linked by horizontal connections. The enhanced response (yellow) is confined to the target curve if it spreads only among neurons with a contour in their RF (grey squares), but not to neurons without RF stimulation (white squares). Orange lines indicate horizontal connections between active neurons that can spread the enhanced response.

B) If the gap between curves is larger, neurons in higher areas with larger RFs (here only V2 is shown) speed up the propagation of the enhanced response. This higher speed is also measured in area V1 because the higher areas provide feedback.

C) The distance between the target and distractor curve determines the level of the visual system where the propagation of the enhanced response makes fastest progress. If the gap is narrow the propagation has to take place in lower areas with smaller RFs at the cost of a decrease in speed.

It is important that neurons in higher areas do not participate in the propagation if their receptive fields fall on multiple curves, because the enhanced response might spill over to the wrong curve, degrading the selectivity of the tracing process. In these instances neurons in lower visual areas, with their smaller receptive fields come into play because they can carry out the process at the required resolution, although at the cost of a lower grouping speed. Figure 7C illustrates the grouping of contour elements at multiple scales and involving neurons at different levels of the cortical hierarchy with different sizes of receptive fields. The correspondence between this neurophysiological model and the growth-cone model is straightforward because the size of the attentional growth cones would correspond to the receptive field size in the cortical area where the tracing process makes fastest progress (compare Figure 6A and 7C).

Alternative models of curve tracing

We will now consider alternative models that have been suggested for contour grouping. Two models that could be ruled out above were the pixel-by-pixel model suggesting that the latency of the attentional modulation depends on arc length of the curve between the fixation point, and the eccentricity model suggesting the latency solely reflects receptive field eccentricity. These two models cannot explain why the latency of the modulation of the responses of neurons with far receptive fields depends on the distance between the target and distractor curve at the critical zone. Moreover, we found that these models do not explain any variance in the data not accounted for by the growth-cone model.

Another model for object-based attention that we considered in the introduction holds that shapes are selected in a competitive interaction in higher shape selective areas that feed back to lower areas to also enhance the response of all the neurons that code the individual contour elements of the relevant shape (Figure 1A). The simplest version of this class of models holds that the competition between shapes is first resolved in higher areas before feedback to lower areas takes place. Our results are not consistent with such a model, since it would predict that all neurons that code the contour elements of one curve should enhance their response at the same time while we observed a systematic progression in modulation latency along the curve. Furthermore, such a model would predict that factors that influence the speed with which the competition between shapes is resolved affects the timing of the modulation of all the lower-level neurons coding the relevant shape, irrespective of the location of their receptive fields. Instead, we found that variations in the configuration at the critical zone only influenced the responses of neurons with far receptive fields and not with close receptive fields. We would

like to stress that although the findings of the present study do not support the *simplest* version of a shape feedback model, they do not exclude a role for feedback from higher visual areas. The neurophysiological implementation of the growth-cone model illustrated in Figure 7 requires feedback connections so that neurons in early visual areas can benefit from the faster propagation in higher visual areas. Furthermore, in a psychophysical study Vecera & Farah (1997) tested observers in a task where they had to decide whether two cues fell on the same or different objects. They demonstrated that grouping of image elements of a familiar object occurs faster than the grouping of elements of the same object shown upside down. This result suggests that feedback from shape selective neurons might indeed facilitate the grouping of contour elements that belong to the shape, because feedback would be stronger for the familiar upright shapes that are better represented in the higher areas than the same shapes shown upside down. Our results demonstrate that besides these putative top-down effects of the higher visual areas, there is also a role to be played by the horizontal connections that spread the response enhancement horizontally according to the lower level Gestalt rules, like good continuation.

The final model that we will consider is the attentional zoom-lens model proposed by Jolicoeur and his colleagues (Figure 1C) (Jolicoeur et al., 1991a; McCormick and Jolicoeur, 1991; McCormick and Jolicoeur, 1994). These authors were the first to suggest that a variably-sized attentional operator might be shifted along the target curve and to hypothesize that the scaling of the zoom-lens could account for the scale invariance of curve-tracing (Jolicoeur and Ingleton, 1991). Our growth-cone model was inspired by the zoom-lens model, and the main difference between models is that attentional modulation is maintained on the initial segments of the target curve in the growth-cone model but not in the zoom-lens model. We found clear evidence that the neurons with a receptive field on the beginning of the target curve maintain the response enhancement and our results therefore do not support this aspect of the zoom-lens model. Our results are in line with psychophysical studies of curve tracing showing that attention gradually spreads along a traced curve but that it does not retract from the initial contour elements (Houtkamp et al., 2003). Attention during curve tracing apparently assumes the shape of the relevant object, which is in accordance with object-based models of attention (Baylis and Driver, 1993; Duncan, 1984; Egly et al., 1994; Kahneman et al., 1992; O'Craven et al., 1999a; Prinzmetal, 1981; Vecera and Farah, 1994). Attention may thereby act to identify all contour elements of an object, binding them together in a coherent representation.

Speed of the spread of attention

The present study is the first to measure the dynamics of the spread of attention within an object representation and we observed that a single shift of the attentional growth-cone requires ~50ms. According to the scheme of Figure 7, this time corresponds to the propagation of the enhanced response from a neuron to a neighbouring one with an adjacent, but non-overlapping receptive field, while neurons with intermediate and partially overlapping receptive fields would enhance their response at intermediate time points as we envision a gradual wave of enhanced activity rather than a discrete, stepwise process. It was previously observed that neurons with adjacent but non-overlapping receptive fields in monkeys' primary visual cortex are separated by 2-3mm (Hubel and Wiesel, 1974) and our results therefore predict that the speed of propagation of the enhanced activity through the horizontal connections equals approximately 5cm/s (i.e. 2.5mm/50ms). It is remarkable that this estimate is in the same range (albeit slightly slower) as the 10cm/s for the horizontal propagation of neuronal activity observed with intracellular recordings in cat visual cortex (Bringuier et al., 1999) and the value of 9-25cm/s observed with voltage-sensitive dye imaging in area V1 of macaque monkeys (Grinvald et al., 1994), while a study using extracellular recordings obtained a slightly higher horizontal propagation speed of 30cm/s in area V1 of monkeys (Girard et al., 2001).

At the same time, our estimate of 50ms per shift is slightly faster (but also in the same range) than the 80-100ms per shift observed in psychophysical studies with human subjects in the curve tracing task (McCormick and Jolicoeur, 1991; McCormick and Jolicoeur, 1994), which would correspond to a speed of approximately 2.5cm/s in the visual cortex. This estimate fits well with the results of a human fMRI study that cortical activity caused by changes in eye dominance during binocular rivalry spreads with a velocity of approximately 2cm/s in area V1 (Lee et al., 2005). We therefore conclude that our estimate of 50ms per shift for the spread of object-based attention is within the same range of estimates derived previously with neurophysiological methods, neuroimaging techniques as well as psychophysics.

It is of interest to compare our results to the delays that are associated with an attention shift from one object to another one. Such a between-object attention shift requires between 140ms and 190ms (Busse et al., 2008; Khayat et al., 2006), which is more time than required for a single shift of the growth cone during curve tracing. This difference in speed presumably reflects the different machinery responsible for within- and between object shifts of attention. Studies of attention shifts between objects usually use an endogenous visual cue to indicate

that attention should be directed elsewhere. This cue first has to be registered in the visual system, to activate neurons in higher areas of the parietal and frontal cortex involved in the control of attention,(Bisley and Goldberg, 2003; Yantis et al., 2002) and these areas then have to feed back to the visual areas to initiate the shift. In the present contour grouping task, however, the response enhancement can spread directly through horizontal connections between adjacent neurons in the visual cortex. In a recent study we found that neurons in area FEF of the frontal cortex also enhance their response if their receptive field falls on the target curve during curve tracing, and that the attentional modulation in area FEF did not occur substantially earlier than that in area V1 (Khayat et al., 2009), which is in accordance with a direct propagation of the enhanced response within the visual cortex.

In conclusion, our results indicate that object-based attention is associated with the spread of an enhanced neuronal response between neurons with adjacent receptive fields. The remarkable consistency of our speed estimate of 50ms per receptive field with the horizontal propagation speed in the visual cortex indicates that it may be worthwhile for future studies to test whether the delays that occur during object-based attention indeed reflect the properties of horizontal connections.

Experimental Procedures

All procedures complied with the NIH Guide for the Care and Use of Laboratory animals and were approved by the institutional animal care and use committee of the Royal Netherlands Academy of Arts and Sciences.

Recording Technique

Two macaque monkeys participated in the experiments. The monkeys underwent two operations under aseptic conditions and general anaesthesia, as described previously (Roelfsema et al., 1998; Roelfsema and Spekreijse, 2001). In a first operation, a gold ring was inserted under the conjunctiva of one eye in order to measure the eye movements with the double magnetic induction technique (Bour et al., 1984), with a sampling rate between 500 and 1000 Hz. In a separate operation, electrodes (40 to 50 teflon-coated platinum-iridium wires per hemisphere) were implanted 1-2 mm below the cortical surface of area V1. In order to detect the multiunit activity, the recorded signal was amplified, band-pass filtered (750-5000 Hz), full-wave rectified, and then low-pass filtered (<200 Hz). The receptive field dimensions were calculated as the extent of the visual field from which responses to a moving

light bar could be elicited. The receptive fields had a median area of 0.6 deg^2 and a mean eccentricity of 2.8 deg.

Behavioral Task

The monkeys sat at a distance of 0.75 cm from a CRT monitor (resolution 1024 × 768, frame rate 70 Hz). A trial started as soon as the monkeys' eye was within a 1 deg × 1 deg window centred on the fixation point (red circle, 0.2° diameter). After 300 ms, the stimuli appeared, but the monkey had to maintain steady fixation (Figure 2). The stimuli consisted of two white curves (luminance 85 cd/m^2) with two red circles at one of their ends and were presented on a black background (luminance 1.5 cd/m^2). In each trial only one of the two curves was connected to the fixation point and is referred to as the target curve. The monkeys had to mentally trace this curve and ignore the other distracter curve. After 600 ms, the fixation point was extinguished and the monkeys made an eye movement towards one of the red circles. An eye movement to the circle located on the target curve was counted as a correct response and was rewarded by a drop of apple juice. To manipulate the difficulty of tracing, the shape of the curves were changed within a small critical zone (blue squares in figure 2B). Within the critical zone, a non-intersection could be gradually transformed to an intersection, under control of a single parameter (gap size for non intersections and angle for intersections). All stimuli (differing in their connection with the fixation point and with intersections and non-intersections) were randomly interleaved and presented equally often.

Data Analysis

Peristimulus time histograms (PSTHs) were computed by averaging the responses across the correct trials and normalizing to the peak response after subtraction of the spontaneous activity. To determine whether a recording site had significant modulation due to attention, the single-trial responses (averaged in a window from 200-500 ms after stimulus onset) to the target curve were compared with responses to the distracter curve (Mann-Whitney *U*-test, α = 0.05). Attention *d*' values (shown in figure 4B and supplementary figure S1) were measured as the mean difference between the responses to the target and distracter curve normalized by the average standard deviation of the two responses. The latency of attentional modulation was determined by fitting a function *f*(t) to the difference between responses to the target and the distracter curve as has been described previously (Roelfsema et al., 2003; Roelfsema et al., 2007). The latency was defined as the time that the fitted function reached 33% of its

maximum value, but other criteria yielded similar results (see Results). A detailed description of the curve fitting method can be found in the Supplementary Material.

Acknowledgements

We thank Victor Lamme for his assistance in the surgeries and Kor Brandsma and Jacques de Feiter for biotechnical assistance. The work was supported by a grant of the HFSP, a grant of the European Union (EU IST Cognitive Systems, project 027198 "Decisions in Motion") and a NWO-VICI grant.

Reference List

Baylis, G.C., and Driver, J. (1993). Visual attention and objects: evidence for hierarchical coding of location. J. Exp. Psychol. Hum. Percept. Perform. *19*, 451-470.

Bisley, J.W., and Goldberg, M.E. (2003). Neuronal activity in the lateral intraparietal area and spatial attention. Science *299*, 81-86.

Bosking, W.H., Zhang, Y., Schofield, B., and Fitzpatrick, D. (1997). Orientation selectivity and the arrangement of horizontal connections in tree shrew striate cortex. J. Neurosci. *17*, 2112-2127.

Bour, L.J., van Gisbergen, J.A., Bruijns, J., and Ottes, F.P. (1984). The double magnetic induction method for measuring eye movement--results in monkey and man. IEEE Trans. Biomed. Eng *31*, 419-427.

Brincat, S.L., and Connor, C.E. (2004). Underlying principles of visual shape selectivity in posterior inferotemporal cortex. Nat. Neurosci. *7*, 880-886.

Bringuier, V., Chavane, F., Glaeser, L., and Fregnac, Y. (1999). Horizontal propagation of visual activity in the synaptic integration field of area 17 neurons. Science *283*, 695-699.

Busse, L., Katzner, S., and Treue, S. (2008). Temporal dynamics of neuronal modulation during exogenous and endogenous shifts of visual attention in macaque area MT. Proc. Natl. Acad. Sci. U. S. A *105*, 16380-16385.

Crundall, D., Dewhurst, R., and Underwood, G. (2008). Does attention move or spread during mental curve tracing? Percept. Psychophys. *70*, 374-388.

Desimone, R., and Duncan, J. (1995). Neural mechanisms of selective visual attention. Annu. Rev. Neurosci. *18*, 193-222.

Duncan, J. (1984). Selective attention and the organization of visual information. J. Exp. Psychol. Gen. *113*, 501-517.

Edelman, S. Line connectivity algorithms for an asynchronous pyramid computer. 2. Comput.Vision Graph.Image Process. 40, 169-187. 1987. Academic Press Professional, Inc. Ref Type: Generic

Egly, R., Driver, J., and Rafal, R.D. (1994). Shifting visual attention between objects and locations: evidence from normal and parietal lesion subjects. J. Exp. Psychol. Gen. *123*, 161-177.

Eriksen, C.W., and St James, J.D. (1986). Visual attention within and around the field of focal attention: a zoom lens model. Percept. Psychophys. *40*, 225-240.

Fukushima, K. A Neural Network for Visual Pattern Recognition. 3. Computer 21, 65-75. 1988. IEEE Computer Society Press.
Ref Type: Generic

Girard, P., Hupé, J.M., and Bullier, J. (2001). Feedforward and feedback connections between area V1 and V2 of the monkey have similar rapid conduction velocities. J Neurophysiol *85*, 1328-1331.

Grinvald, A., Lieke, E.E., Frostig, R.D., and Hildesheim, R. (1994). Cortical point-spread function and long-range lateral interactions revealed by real-time optical imaging of macaque monkey primary visual cortex. J. Neurosci. *14*, 2545-2568.

Grossberg, S. (1999). The link between brain learning, attention, and consciousness. Conscious. Cogn *8*, 1-44.

Grossberg, S., and Raizada, R.D. (2000). Contrast-sensitive perceptual grouping and object-based attention in the laminar circuits of primary visual cortex. Vision Res. *40*, 1413-1432.

Houtkamp, R., Spekreijse, H., and Roelfsema, P.R. (2003). A gradual spread of attention during mental curve tracing. Percept. Psychophys. *65*, 1136-1144.

Hubel, D.H., and Wiesel, T.N. (1974). Uniformity of monkey striate cortex: a parallel relationship between field size, scatter, and magnification factor. J. Comp Neurol. *158*, 295-305.

Jolicoeur, P., and Ingleton, M. (1991). Size invariance in curve tracing. Mem. Cognit. *19*, 21-36.

Jolicoeur, P., Ullman, S., and Mackay, M. (1991b). Visual curve tracing properties. J. Exp. Psychol. Hum. Percept. Perform. *17*, 997-1022.

Jolicoeur, P., Ullman, S., and Mackay, M. (1991a). Visual curve tracing properties. J Exp. Psychol. Hum. Percept. Perform. *17*, 997-1022.

Kahneman, D., Treisman, A., and Gibbs, B.J. (1992). The reviewing of object files: object-specific integration of information. Cognit. Psychol. *24*, 175-219.

Kanwisher, N., and Driver, J. (1997). Objects, attributes, and visual attention: which what and where. Ref Type: Generic. Curr Dir Psychol Sci *1*, 26-31.

Khayat, P.S., Pooresmaeili, A., and Roelfsema, P.R. (2009). Time-Course of Attentional Modulation in the Frontal Eye Field During Curve Tracing. J. Neurophysiol.

Khayat, P.S., Spekreijse, H., and Roelfsema, P.R. (2006). Attention lights up new object representations before the old ones fade away. J. Neurosci. *26*, 138-142.

Koffka,K. (1935). Principles of Gestalt Psychology (New York: Harcourt, Brace and Compony).

Lee, S.H., Blake, R., and Heeger, D.J. (2005). Traveling waves of activity in primary visual cortex during binocular rivalry. Nat. Neurosci. *8*, 22-23.

Li, W., Piech, V., and Gilbert, C.D. (2006). Contour saliency in primary visual cortex. Neuron *50*, 951-962.

McCormick, P.A., and Jolicoeur, P. (1991). Predicting the shape of distance functions in curve tracing: evidence for a zoom lens operator. Mem. Cognit. *19*, 469-486.

McCormick, P.A., and Jolicoeur, P. (1994). Manipulating the shape of distance effects in visual curve tracing: further evidence for the zoom lens model. Can. J Exp. Psychol. *48*, 1-24.

Moran, J., and Desimone, R. (1985). Selective attention gates visual processing in the extrastriate cortex. Science *229*, 782-784.

O'Craven, K.M., Downing, P.E., and Kanwisher, N. (1999a). fMRI evidence for objects as the units of attentional selection. Nature *401*, 584-587.

O'Craven, K.M., Downing, P.E., and Kanwisher, N. (1999b). fMRI evidence for objects as the units of attentional selection. NATURE *401*, 584-587.

Oram, M.W.a.P.D.I. Modeling visual recognition from neurobiological constraints. Neural Netw 7[6-7], 945-972. 1994.
Ref Type: Generic

Posner, M.I. (1980). Orienting of attention. Q. J. Exp. Psychol. *32*, 3-25.

Prinzmetal, W. (1981). Principles of feature integration in visual perception. Percept. Psychophys. *30*, 330-340.

Roelfsema, P.R. (2006). Cortical algorithms for perceptual grouping. Annu. Rev. Neurosci. *29*, 203-227.

Roelfsema, P.R., Khayat, P.S., and Spekreijse, H. (2003). Subtask sequencing in the primary visual cortex. Proc. Natl. Acad. Sci. U. S. A *100*, 5467-5472.

Roelfsema, P.R., Lamme, V.A., and Spekreijse, H. (1998). Object-based attention in the primary visual cortex of the macaque monkey. Nature *395*, 376-381.

Roelfsema, P.R., Lamme, V.A., and Spekreijse, H. (2000). The implementation of visual routines. Vision Res. *40*, 1385-1411.

Roelfsema, P.R., and Singer, W. (1998). Detecting connectedness. Cereb. Cortex *8*, 385-396.

Roelfsema, P.R., and Spekreijse, H. (2001). The representation of erroneously perceived stimuli in the primary visual cortex. Neuron *31*, 853-863.

Roelfsema, P.R., Tolboom, M., and Khayat, P.S. (2007). Different processing phases for features, figures, and selective attention in the primary visual cortex. Neuron *56*, 785-792.

Schmidt, K.E., Kim, D.S., Singer, W., Bonhoeffer, T., and Lowel, S. (1997). Functional specificity of long-range intrinsic and interhemispheric connections in the visual cortex of strabismic cats. J. Neurosci. *17*, 5480-5492.

Scholte, H.S., Spekreijse, H., and Roelfsema, P.R. (2001). The spatial profile of visual attention in mental curve tracing. Vision Res. *41*, 2569-2580.

Sheinberg, D.L., and Logothetis, N.K. (2001). Noticing familiar objects in real world scenes: the role of temporal cortical neurons in natural vision. J. Neurosci. *21*, 1340-1350.

Tanaka, K. (1993). Neuronal mechanisms of object recognition. Science *262*, 685-688.

Thorpe, S., Fize, D., and Marlot, C. (1996). Speed of processing in the human visual system. Nature *381*, 520-522.

Van der Velde, F., and de Kamps, M. (2001). From knowing what to knowing where: modeling object-based attention with feedback disinhibition of activation. J. Cogn Neurosci. *13*, 479-491.

Vecera, S.P., Behrmann, M., and Filapek, J.C. (2001). Attending to the parts of a single object: part-based selection limitations. Percept. Psychophys. *63*, 308-321.

Vecera, S.P., Behrmann, M., and McGoldrick, J. (2000). Selective attention to the parts of an object. Psychon. Bull. Rev. *7*, 301-308.

Vecera, S.P., and Farah, M.J. (1994). Does visual attention select objects or locations? J. Exp. Psychol. Gen. *123*, 146-160.

Vecera, S.P., and Farah, M.J. (1997). Is visual image segmentation a bottom-up or an interactive process? Percept. Psychophys. *59*, 1280-1296.

Wertheimer, M. Untersuchungen zur Lehre von der Gestalt II. 350. 301. Psychologische Forschung 4. 1923.
Ref Type: Generic

Yantis, S., Schwarzbach, J., Serences, J.T., Carlson, R.L., Steinmetz, M.A., Pekar, J.J., and Courtney, S.M. (2002). Transient neural activity in human parietal cortex during spatial attention shifts. Nat. Neurosci. *5*, 995-1002.